

Distinguishing quasiperiodic from random order in high-resolution TEM images

Dieter Joseph

Laboratory of Atomic and Solid State Physics, Clark Hall, Cornell University, Ithaca, New York 14853-2501

Stefan Ritsch*

Laboratory of Solid State Physics, Swiss Federal Institute of Technology Zürich (ETHZ), 8093 Zürich, Switzerland

Conradin Beeli

Interdepartmental Center of Electron Microscopy, Swiss Federal Institute of Technology Lausanne (EPFL), 1015 Lausanne, Switzerland

(Received 19 September 1996)

We investigate the question of whether an experimental tiling that was constructed by superimposition onto a high-resolution transmission electron microscopy (HRTEM) image belongs to the ideal quasiperiodic or to the random tiling class. To answer this question, statistical arguments and our method are applied to different decagonal Al-Co-Ni phases. This method allows us to distinguish between both classes even if tiling errors and poor statistics are involved. A possible stabilization mechanism is discussed for a high-temperature phase that is ideally quasiperiodic. [S0163-1829(97)01813-4]

I. INTRODUCTION

The science of quasicrystals is a very lively field. Up to now, a few hundred chemically different alloys are known which show crystallographically forbidden symmetries. The publication of the discovery of icosahedral quasicrystals in 1984¹ was immediately followed by the description of dodecagonal quasicrystals.² Shortly after that, the decagonal phases were discovered³ and the octagonal quasicrystals followed in 1987.⁴ These four different classes have now found a supplement in the discovery of pentagonal phases.^{5,6} Except for the icosahedral phases all other symmetry classes belong to the so-called quasiperiodic T phases, i.e., they consist of periodically stacked aperiodic planes and can be classified with the help of their translation periods in the periodic direction (within their symmetry classes).

The experimental discovery of quasicrystals was accompanied by much theoretical work. From the beginning, theoreticians mainly focused on structural aspects of quasiperiodicity: Besides some other proposals, two-dimensional (2D) and 3D quasiperiodic tilings were used to describe the geometrical structure of the new materials. For several years, the physical properties became more and more important. Even before the above-mentioned experimental discoveries, the two most famous quasiperiodic tilings, the (2D) Penrose tiling⁷ and the (3D) Ammann-Kramer tiling,⁸ were known. These tilings can be produced by an irrational cut through a higher-dimensional lattice. Therefore, their whole geometrical structure is deterministic, in the sense that one can exactly calculate the surrounding of every point in real space. Today both tilings are the prototypes of the so-called ideal quasiperiodic tilings in 2D and 3D, respectively, and they started a whole field of mathematical^{9,10} and physical interest.¹¹

Shortly after the experimental discovery, Elser¹² pointed out that one could relax the construction of the ideal tilings without disturbing their key features. If one takes, e.g., the same tiles as in the ideal case, but now rearranges them face

to face in a random manner, one would get the same averaged symmetry in Fourier space and only a slightly different form of the Bragg intensities and some background modifications. The differences of both, ideally quasiperiodic and random tilings, are so tiny, that even today, 12 years later, it is hard or even impossible for an experimentalist to answer the question, whether the structure of a sample belongs to the class of the ideal quasiperiodic tilings or to the class of the so-called random tilings.

In order to distinguish between quasiperiodic and random tilings one must have excellent samples (better than those of most crystals) and must look at the form of the \mathbf{q} dependence of the experimental Bragg peaks near their bottom. Another approach which is possible, at least in 2D, is to superimpose tilings onto high-resolution transmission electron microscope (HRTEM) images and to investigate the nature of the resulting tilings. The main problems associated with this alternative method are the poor statistics and the existence of (tiling) defects (similar but more crucial than in crystals) which makes a decision between both tiling classes hard and often impossible.

Nevertheless, the physical properties of both classes lead to certain expectations: The ideal quasiperiodic tilings are thought to be stabilized energetically. On the level of the tilings this can be achieved with the so-called matching-rules¹³ or tiling cluster-models¹⁴ and, on the level of real atomic arrangements, with chemical order of the atoms on the constituent clusters.¹⁵ The random tiling ensembles are thought to be stabilized by their (positive) entropy density.¹⁶ Therefore, one would expect that at least in the high-temperature regime the random tiling hypothesis should be favored. However, there are a few theoretical tools to investigate these questions.

This is the point we wish to address. Starting from the situation that experimental tilings superimposed onto HRTEM images are available, a detailed analysis of those tilings is presented with respect to the question whether they belong to the ideal quasiperiodic or to the random tiling scenario,

i.e., we want to say which one is the better idealization for the given tiling. Different theoretical tools of investigation are compared and an application of our method¹⁷ to experimental data is presented. This method does not focus on the very specific kind of tiling or at tiling defects which can be involved, but on statistical correlations of the data only. The method is applied together with conventional ones to variants of the decagonal or pentagonal phases of Al-Co-Ni quasicrystals.

This paper is subdivided as follows: In Sec. II, the main features of the different phases of quasicrystalline Al-Co-Ni are given and the superimposed tilings and their projections into the perpendicular (internal) space are presented. This will be brief and focused on the relevant topics. For a detailed description of the data refer to the original publications cited. In Sec. III, the different methods of investigation of the tilings are introduced and are applied to the data. In Sec. IV, a discussion is presented with respect to the question which stabilization mechanism is most probable in order to explain the results of the analysis.

II. THE EXPERIMENTAL DATA

Besides the icosahedral quasicrystals the decagonal phases (*D* phases) were the subject of the most intense experimental studies. This is due to the fact that the first stable quasiperiodic *T* phases were decagonal and that it was possible to increase the quality of the samples to a high degree. In the course of a redetermination of the Al-Co-Ni phase diagram¹⁸ it was realized that the field of the *D* phase has to be subdivided into several regions with different states of structural order. Up to now, there are at least six different regimes:

(1) The so-called basic Ni-rich decagonal phase.¹⁹

The tenfold diffraction pattern shows an unusually large amount of weak reflections up to q values of 1 \AA^{-1} . Almost no diffuse scattering intensity is present in the ten and in the twofold patterns. It is a high-temperature phase with a period length of 4.1 \AA along the tenfold axis only stable for temperatures above $800 \text{ }^\circ\text{C}$. HRTEM images taken from wedge-shaped grains show decagonal contrasts of atomic clusters 20 \AA in diameter. The centers of these clusters can be used as the vertices of a superimposed tiling with a unique tile edge length of 20 \AA . Taking the usual fivefold star as a basis, the resulting pentagon-star tiling can be lifted into internal space (see Fig. 1). It is even possible to apply a semidecomposition rule²⁰ to the tiling to obtain a 12.4 \AA (see Fig. 2) and a 32.4 \AA version of the tiling.¹⁹

(2) Another basic decagonal phase is present on the Co-rich side of the *D*-phase region (not considered here).

(3) The so-called type-I superstructure.^{21,22}

The tenfold diffraction pattern of this decagonal superstructure shows besides the basic reflections two additional types of satellites (*S1* and *S2*). The superstructure reflections have $1/5$ integer indices and are, e.g., found at the centers of the pentagons formed by the strong basic reflections. Additional diffuse layers visible in the twofold diffraction patterns suggest a doubled period of 8.2 \AA . Type I is a low-temperature phase which transforms at high temperatures into the *S1*-type phase (see below). HRTEM images show atom clusters of 20 \AA diameter with a pentagonal contrast

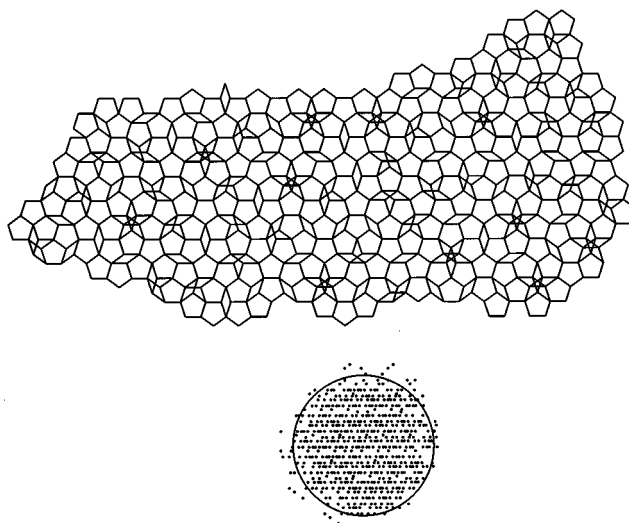


FIG. 1. 20 \AA tiling and internal coordinates of the basic Ni-rich phase (sample: $\text{Al}_{70}\text{Co}_{11}\text{Ni}_{19}$, annealed at $1050 \text{ }^\circ\text{C}$, 12 h).

around the center. The corresponding tiling consists of rhombi and hexagons (see Fig. 3) with 20 \AA edge length. In this tiling every second cluster core has the same orientation, while adjacent neighbors having a distance of 20 \AA from each other change by 180° . It is worthwhile to mention that the *S1* and *S2* satellites can be produced by a kinematical Fourier-transformation (FT) of a Penrose rhombus tiling alone. No complicated decoration but only δ scatterers on the vertices are necessary (see Ref. 23).

(4) The so-called *S1* superstructure.^{22,24}

S1 is the high-temperature phase of type I. The tenfold diffraction pattern of *S1* is essentially the same as for type I but only basic reflections and *S1* satellites remain. It has a period of 8.2 \AA in the periodic direction and can make transformations into all other decagonal Al-Co-Ni phases as a function of temperature and/or composition. HRTEM images again show atom clusters with pentagonal cores which have an antiparallel orientation relationship along the edges of the tiling as explained for type I. (Exceptions from this order have been observed for a Co-rich *S1* state only.) The corre-

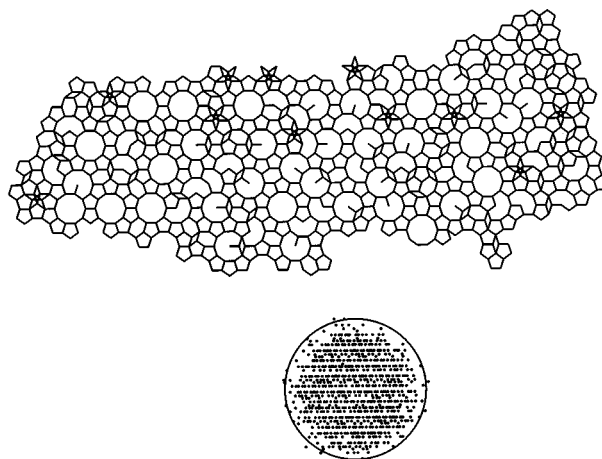


FIG. 2. Decomposed 12.4 \AA tiling and internal coordinates of the basic Ni-rich phase (the same sample as in Fig. 1).

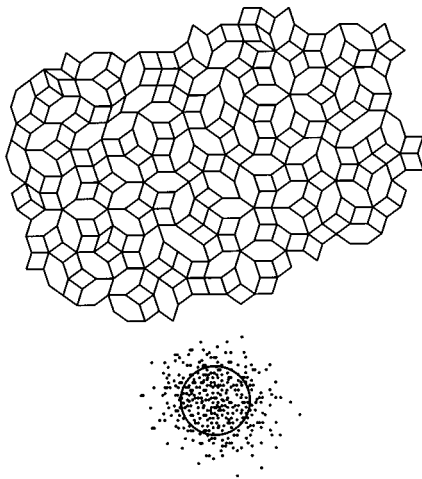


FIG. 3. Tiling and internal coordinates of the type-I superstructure (sample: $\text{Al}_{70}\text{Co}_{15}\text{Ni}_{15}$, cooled from the melt with 5 K/min).

sponding tiling mainly consists of hexagons, kidney-shaped (or bananas), S-shaped tiles, and even larger fractions of entire decagons (see Fig. 4).

(5) The so-called type-II superstructure.²²

The tenfold diffraction pattern shows additional reflections located on ring arrangements of small pentagons around the strong reflections. Additionally, ten diffuse spots surround the strong ones. Different from type I, the satellites of type II have 1/2 integer indices. The twofold diffraction patterns show diffuse layers and a period of 8.2 Å. Type II is a low-temperature phase which can transform into the basic Co-rich type or the S1 superstructure at higher temperatures. Corresponding HRTEM images show 20 Å clusters with pentagonal cores. The superimposed tiling consists of pentagons, rhombi, and hexagons (see Fig. 5). In this case the pentagonal cores reveal an antiparallel ordering as far as possible for a pentagonal distribution.

(6) The one-dimensionally periodic fivefold phase (Ref. 6).

The distribution of spots in the diffraction pattern is ten-

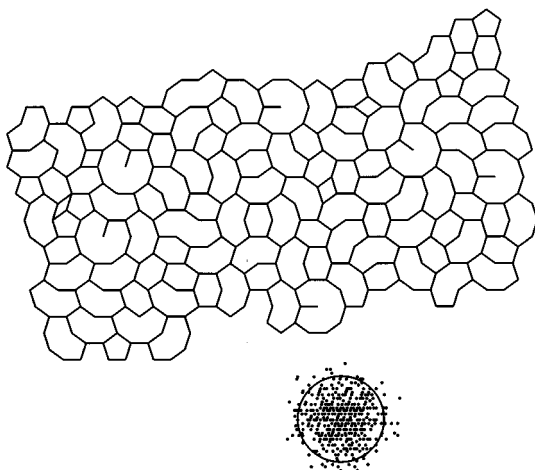


FIG. 4. Tiling and internal coordinates of the S1 superstructure (sample: $\text{Al}_{72.5}\text{Co}_{13.5}\text{Ni}_{14}$, annealed at 900 °C, 2 days).

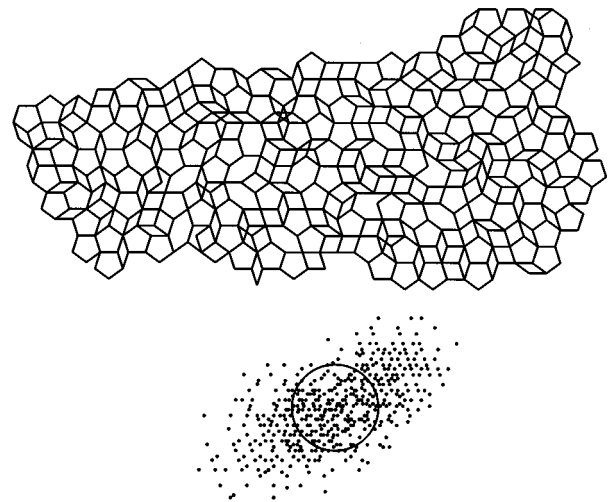


FIG. 5. Tiling and internal coordinates of the type-II superstructure (found in the same sample as in Fig. 3).

fold but the distribution of the intensities reveals only fivefold symmetry. This is due to dynamical scattering effects in the sample which lead to a break of the tenfold symmetry. The twofold patterns have diffuse layers and a period of 8.2 Å. HRTEM images show 20 Å clusters with pentagonal cores which have in this case only one single orientation. The corresponding tiling consists of pentagons, rhombi, kidneys, and deformed hexagons (see Fig. 6). Only dynamical diffraction can reproduce the fivefold symmetry in the intensity distribution. For preparation of samples and further details refer to the publications cited.

III. THE METHODS OF THE TILING ANALYSIS

The experimental tilings which were introduced in the previous section show significant differences. Nevertheless, it is not possible to recognize at first glance whether one of these tilings is an ideal quasiperiodic one. Ideally quasiperiodic and random tilings cannot easily be distinguished in real space due to tiling errors which appear in every real structure. It is necessary to project the tilings into internal space

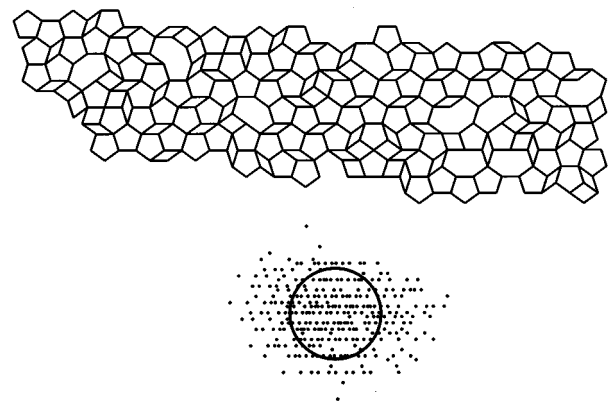


FIG. 6. Tiling and internal coordinates of the one-dimensionally periodic fivefold phase (sample: $\text{Al}_{72.5}\text{Co}_{20}\text{Ni}_{7.5}$, annealed at 1050 °C, 10 h).

since the correlations of the positions of the vertices in real space are coded in internal space. Therefore, Figs. 1–6 present also the coordinates in internal space together with the outer circle of the acceptance domains of the corresponding ideal quasiperiodic tiling. All considerations below will be done in internal space.

A. The variance test

The first (conventional) analysis is motivated by the hydrodynamic approximation of tilings in the random tiling hypothesis.¹⁶ The correlations of the internal space coordinates are connected with the phasonic entropy density of the corresponding tiling ensemble. In particular, the variance $\overline{h^2}$ of the distribution of the coarse-grained internal coordinates h_i behaves like

$$\begin{aligned} 1D, \quad \overline{h^2} &\sim N, \\ 2D, \quad \overline{h^2} &= \frac{1}{2\pi K_{\text{eff}}} \ln(N) + b, \\ 3D, \quad \overline{h^2} &\sim \text{const}, \end{aligned} \quad (1)$$

where K_{eff} is a combination of elastic constants, N is the number of vertices of the patch, and b is an additional constant due to integration of the elastic tensor in momentum space. The variance diverges linearly with the system size in 1D (equal to a random walk), logarithmically in 2D and is bounded in 3D random tilings. 2D is in a sense a critical dimension because of its logarithmic behavior. In comparison, the variances of the ideal quasiperiodic tilings are always constant, independent of the system size (neglecting fluctuations due to small patch sizes) and dimension. Therefore, in 2D one could try a test of the different behavior of $\overline{h^2}$ as a function of the patch size ignoring the influence of the third (periodic) dimension possibly disturbing the 2D behavior. This has already been tried several times.^{25,26}

An experimentalist does not have a lot of tilings to average. Thus, one has to consider the experimental tiling as one (representative) snapshot out of the tiling ensemble. In order to obtain the patch size dependence of the variance $\overline{h^2}$ larger and larger circles have to be cut out of the experimental tiling. Accordingly, one has to deal with large statistical fluctuations. The next problem is that the experimental tilings were constructed from images obtained from wedge-shaped grains. Therefore, the tilings are lengthy rather than circular. Monte Carlo simulations on random tilings show that this lengthy shape reduces $\overline{h^2}$ on the average.

But the major problem is the poor statistics. Most experimental tilings have a few hundred vertices only. Below one hundred the statistics is too low to determine anything with certainty. There might be only half a decade which remains for statistical tests. That is far from being enough to test a logarithmic divergence.

Figures 7 and 8 show, on a logarithmic scale, the variances of the different tilings of the Al-Co-Ni phases presented in Figs. 1–6. If one neglects the influence of the third (periodic) dimension, theory predicts a linear dependence on this scale, the slope of which determines the combined elastic constant K_{eff} . A slope of zero corresponds to an ideal quasiperiodic tiling. Altogether, there is one common fea-

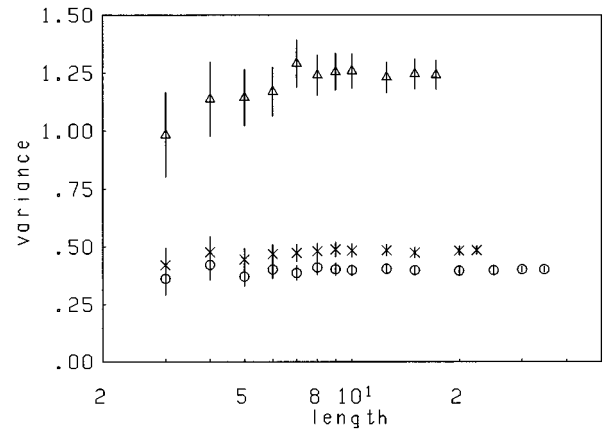


FIG. 7. Variance $\overline{h^2}$ of the internal coordinates of three tilings as a function of patch size: x indicates basic Ni-rich, O is decomposed basic Ni-rich, Δ is type-I.

ture: The statistical errors of $\overline{h^2}$ are so large that one could, in principle, successfully fit many different functions to the data. For a quantitative interpretation statistical tests have to be applied. However, the result would then involve confidence levels, which is not really helpful.

The only certain tendency to be noticed, is the (extremely) linear (and bounded) behavior of $\overline{h^2}$ of the basic Ni-rich tilings (see Fig. 7). Their variances do not at all show any dependence on the system size, despite the low number of vertices. Therefore, one can suggest that the corresponding tilings do not belong to the random type. In comparison to this behavior, all the other variances seem to have a rising character. But the only definite statement is that these variances are generally larger than that of the basic Ni-rich tilings. Since the variance of the tiling of the S1 phase is only weakly rising, it is difficult to decide with this test to which tiling class it belongs. Figure 8 shows $\overline{h^2}$ of the left part of the vertices of Fig. 5 (type II) only. These vertices correspond to the left part of the stretched cloud of internal coordinates. If the whole data were used a tremendous rise and a decline of the variance would result. This is an indication that Fig. 5 consists of two domains of the material. This is

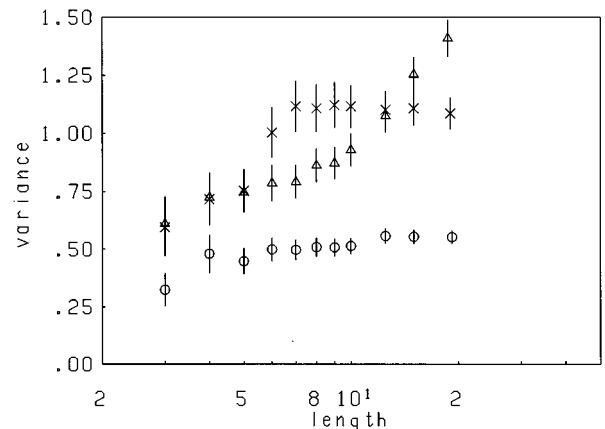


FIG. 8. Variance $\overline{h^2}$ of the internal coordinates of three tilings as a function of patch size: x indicates type-II, O is S1, Δ is the fivefold phase.

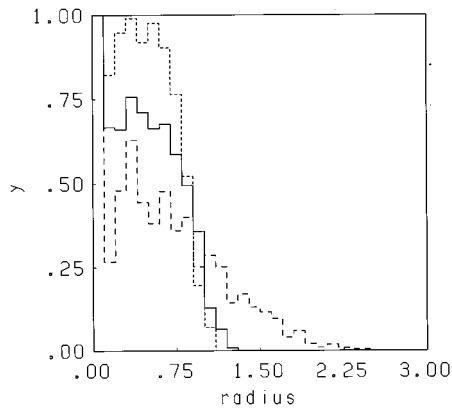


FIG. 9. Radius dependence of the internal coordinates of three tilings: (a) full line: basic Ni-rich, (b) fine dashed line: decomposed basic Ni-rich, (c) dashed line: type-I.

also corroborated by the shape of the internal coordinate distribution. The domain boundary can be recognized in Fig. 5 at the two defects of the tiling in the middle right part of the tiling. A similar behavior is found for the fivefold phase.

B. The R -dependence test

Another possibility to distinguish the two tiling classes is to look at the radius dependence of their internal coordinates. An ideal quasiperiodic tiling has an acceptance domain which is dense and uniformly filled (subdivided into translation classes). It reveals the symmetry of the tiling: pentagons, decagons, octagons, dodecagons, etc. Considering the different decagonal tilings, pentagons and decagons occur as acceptance domains. If the radial dependence of such an acceptance domain is plotted, it is constant up to the inner circle of the domain and decreases rapidly to zero at the outer circle. A random tiling has a Gaussian distribution in internal space and consequently shows an exponential decrease in the radial distribution.

Figures 9 and 10 show the different radial dependences for the Al-Co-Ni samples. The radial dependence of the basic Ni-rich tilings [Figs. 9(a) and 9(b)] shows a significant plateau and a rapid decrease. Accordingly, one can suggest an acceptance domain of an ideal quasiperiodic tiling disturbed

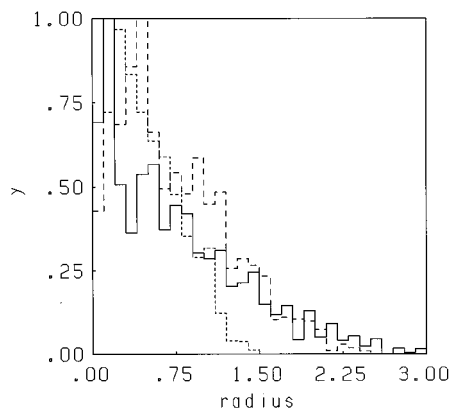


FIG. 10. Radius dependence of the internal coordinates of three tilings: (a) full line: type-II, (b) fine dashed line: S1, (c) dashed line: fivefold phase.

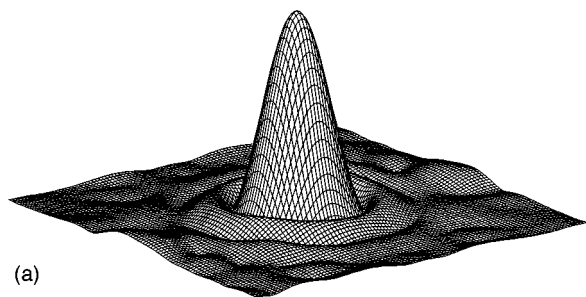
by tiling errors. All the other radial dependences suggest an exponential decrease which would correspond to the random tiling scenario. Nevertheless, the statistics is again the limiting factor also in this test. The relative error bars (not shown here to avoid confusion) are as large as in Figs. 7 and 8 because one has to subdivide the data into bins.

C. The FT test

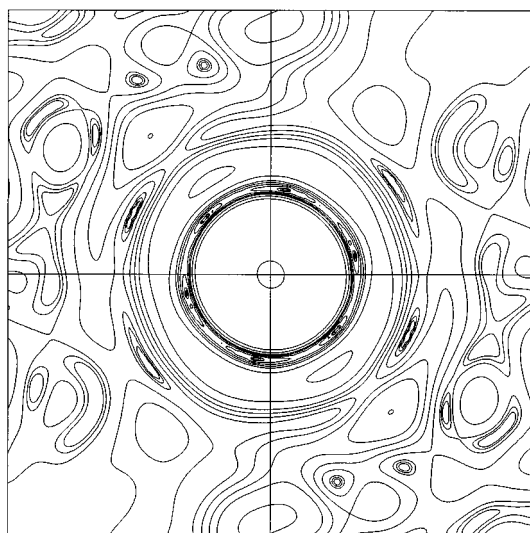
The main disadvantage of both tests, the variance and the R -dependence test, is the poor statistics which will always be present in experimental tilings. To give a more reliable answer one has to enlarge the patches to the size of at least a few thousand vertices. The first test was motivated by the hydrodynamic description of random tilings: the variance is correlated to the entropy of the tiling ensemble, and thus to the free energy. The latter test looks at the differences in the shape of the internal space. One can combine both tests and go even further. The experimental tiling contains much more information because it includes the whole distribution of the internal coordinates with all its correlations. The variance is only the second statistical moment of this distribution. One possibility to use *substantially more* information is the inspection of *all* statistical moments. The simplest way of doing this is achieved through the Fourier transformation (FT) of the whole distribution of the coordinates in internal space. The FT is the generating function of the statistical moments of a distribution, i.e., the moments appear in the coefficients of the Taylor expansion of the FT around $k=0$ (Ref. 27 or any other textbook on probability theory). Therefore, the FT of the distribution of the coordinates in internal space or the FT of the pair-correlation function of these coordinates is a better tool than the above tests to differentiate between 2D ideal quasiperiodic and random tilings. This has already been shown in Monte Carlo simulations of toy models like the octagonal Ammann-Beenker tilings.¹⁷

What do we expect for both tiling classes?

The ideal quasiperiodic tiling has dense and uniformly filled acceptance domains. In the case of ordinary decagonal tilings these domains consist of pentagons and decagons. For simplicity we approximate these domains by a circle with the same area. The FT of a filled circle of radius R is $(2\pi R/k)J_1(kR)$, where J_1 is the first Bessel function and k is the absolute value of the wave vector. On the other hand, the perpendicular coordinates of a random tiling approximate a Gaussian distribution. This is, of course, transformed into another Gaussian under FT. Therefore, an oscillating function in the case of the ideal tilings is obtained. These oscillations correspond to the special long-distance correlations in ideal tilings. A Gaussian which results in the case of the random tiling indicates the absence of these special long-distance correlations. This should be true, even if tiling defects and poor statistics are involved. Of course, we cannot expect an exact $(2\pi R/k)J_1(kR)$ dependence in the case of the ideal tilings: we have made a circle approximation for a polygonal shape. Furthermore, the experimental tilings represent finite systems. Therefore, a discrete FT must be applied, resulting in an imaginary function which should reveal the symmetry of the tiling. Nevertheless, the absolute value of the FT will show besides the symmetry also the corresponding oscillations.



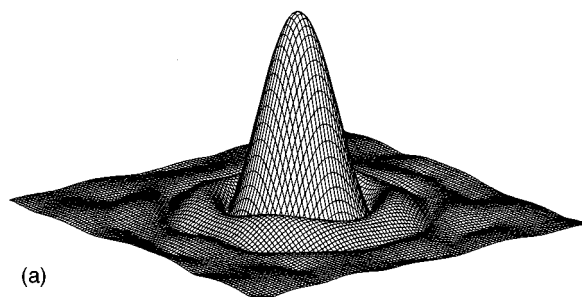
(a)



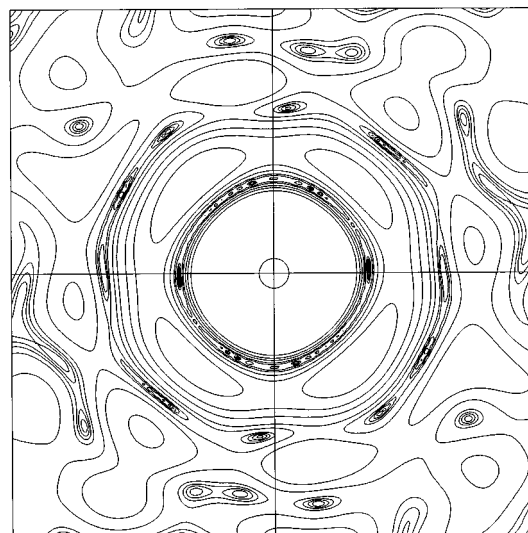
(b)

FIG. 11. Absolute value of the Fourier transformation of the internal coordinates of the basic Ni-rich phase (Fig. 1) and its contour plot.

Figures 11–16 show the absolute value of the FT of the internal coordinates of the different Al-Co-Ni samples and the corresponding contour plots. The latter focus on the regions of relative strength below 10%. The figures reveal the characteristic differences of the samples. Note that this time nearly all available statistical information is used, e.g., the variance can be seen in the width of the central peak: The larger the variance, the narrower the peak. Therefore, in the case of the basic Ni-rich tilings (Figs. 1 and 2), not only the second moment of the distribution but *all* correlations in internal space favor the ideal quasiperiodic tiling picture (see Figs. 11 and 12). This can be seen in the oscillating character of the FT. The existence of a first and a second maximum (besides the central peak) indicates that *long-distance correlations* of ideally quasiperiodic tilings are present in internal space and, therefore, also in the real-space tilings. The only possible different explanation is a super-random tiling with a long bond length decorated in an ideal manner. Thus, the indexed experimental tiling would be just a decoration of the super-random tiling rather than a real tiling itself. The FT of the convolution of the decoration with a narrow Gaussian (super-random tiling) would also result in an oscillating function. Nevertheless, the corresponding bond length of the super-random tiling must be very long and it makes no sense to perform an analysis if only a few super-tiles remain. On the other hand, one should find a clear signature of the super-



(a)



(b)

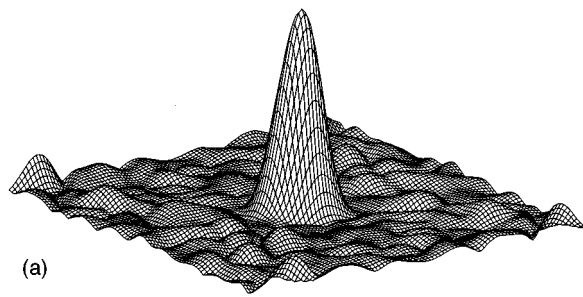
FIG. 12. Absolute value of the Fourier transformation of the internal coordinates of the decomposed tiling of the basic Ni-rich phase (Fig. 2) and its contour plot.

tiling in the diffraction data and in the HRTEM images. This is not the case in the basic Ni-rich phase. Therefore, this possibility can be ruled out. The geometric nature of the tilings superimposed onto HRTEM images of the basic Ni-rich phase is clearly ideally quasiperiodic on the scale of the tilings and not random.

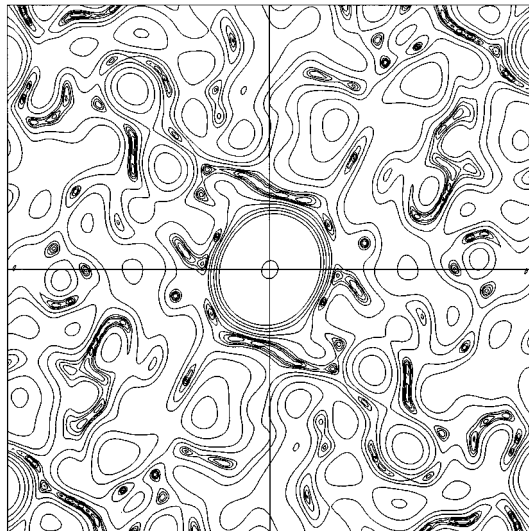
In contrast to these plots of the basic Ni-rich phase all other tilings favor the random tiling hypothesis. Although maxima are visible, they do not form the characteristic ring-like maxima of Figs. 11 and 12. These maxima are fluctuations due to poor statistics. Therefore we can conclude that the statistically available information of the tilings obtained from different samples of Al-Co-Ni lead to the results summarized in Table I. Note that only the geometrical informa-

TABLE I. Geometrical nature of the tilings superimposed onto the different decagonal phases of Al-Co-Ni.

Type	Geometrical nature of tiling
Basic Ni-rich	Ideal quasiperiodic
Type-I	Random
S1	Random
Type-II	Random
Fivefold	Random
Basic Co-rich	Random (not presented here)



(a)



(b)

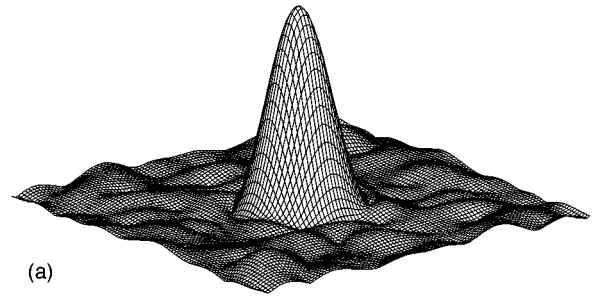
FIG. 13. Absolute value of the Fourier transformation of the internal coordinates of type-I superstructure (Fig. 3) and its contour plot.

tion of the tilings superimposed onto HRTEM images has been analyzed.

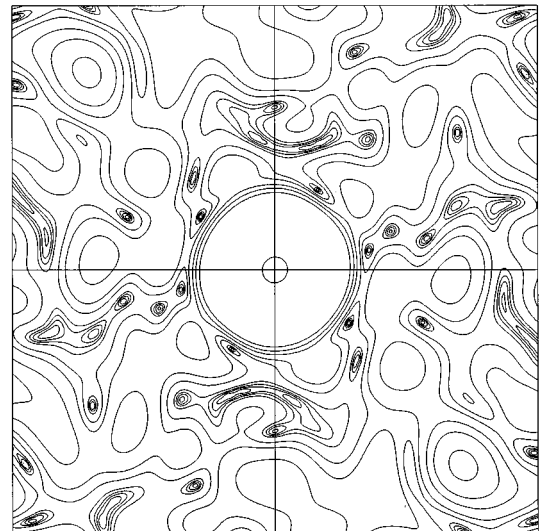
IV. DISCUSSION AND CONCLUSION

The results of the geometrical analysis, which is summarized in Table I, need some comments. The *S1* superstructure is a high-temperature phase. Its tiling seems to be quite a good random tiling (at least) near equilibrium. It consists of hexagons, polygonal kidney-shaped, and S-shaped tiles. All of these tiles can be decomposed into pentagons and/or rhombi. Therefore, one can assume that possible inner vertices of these tiles cannot be seen due to phason-related stacking disorder.²⁸ The twofold diffraction patterns indeed show diffuse layers perpendicular to the tenfold axis, indicating this stacking disorder. A simulation²⁸ of the influence of stacking disorder in corresponding HRTEM images supports this argument. If, for example, inside a hexagon the cluster at the inner vertex flips to the second possible position after approximately half of the specimen thickness, the corresponding wheel contrast which marks the clusters (and thus the vertices of the tiling) is extinguished. This phason flip of one column of the atom clusters corresponds to a local linear stacking defect.

The type-I sample has a wide-spread internal cloud (see Fig. 3). Since it is a low-temperature phase, it might be as-



(a)



(b)

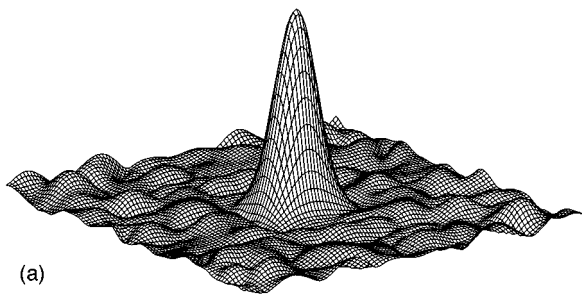
FIG. 14. Absolute value of the Fourier transformation of the internal coordinates of the *S1* superstructure (Fig. 4) and its contour plot.

sumed that it corresponds to a quenched random tiling far from equilibrium. The phason fluctuations of the random phase are frozen in due to the low temperature.

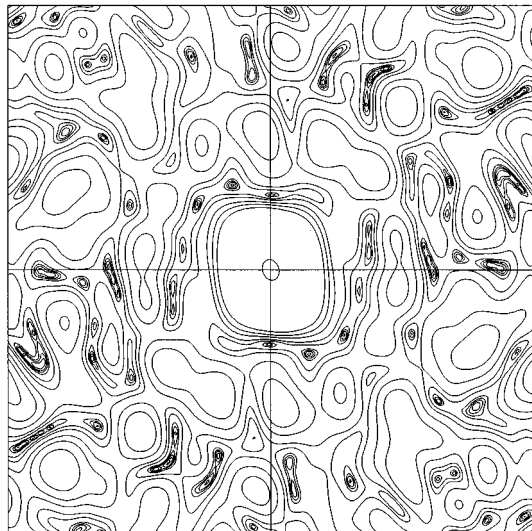
The really surprising result of the geometrical analysis of the tilings is the finding that the basic Ni-rich type corresponds—from a geometrical point of view—to an ideal quasiperiodic tiling. On the one hand, it is a pure high-temperature phase which decays below 800 °C into the *S1* phase plus crystalline phases.¹⁸ On the other hand, it can be the high-temperature phase of *S1*. This means a transformation from a random tiling to an ideal quasiperiodic structure by increasing the temperature. This is indeed not the expected process. A transformation from ideal quasiperiodic to random with increasing temperature would make sense in the random tiling hypothesis.

In the following we will propose two possible explanations for this surprising behavior:

The first is that the effect is only due to the projection which is obtained in a HRTEM image. This projection along the periodic direction could eliminate (by averaging) the randomness of a periodic stack of random tilings and a somewhat more quasiperiodic image would remain.²⁹ A model like this will have stacking disorder and an occupation density of the atomic columns below one. There are two counterarguments against this explanation. The first one is: why does this happen in the basic Ni-rich samples only and not in



(a)



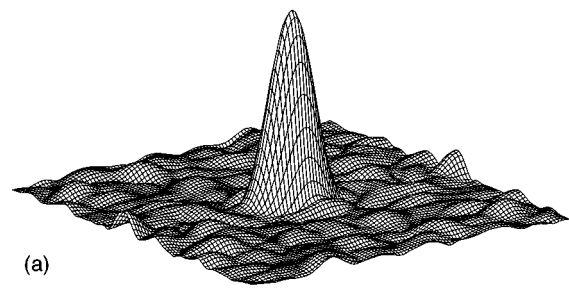
(b)

FIG. 15. Absolute value of the Fourier transformation of the internal coordinates of type-II superstructure (Fig. 5) and its contour plot.

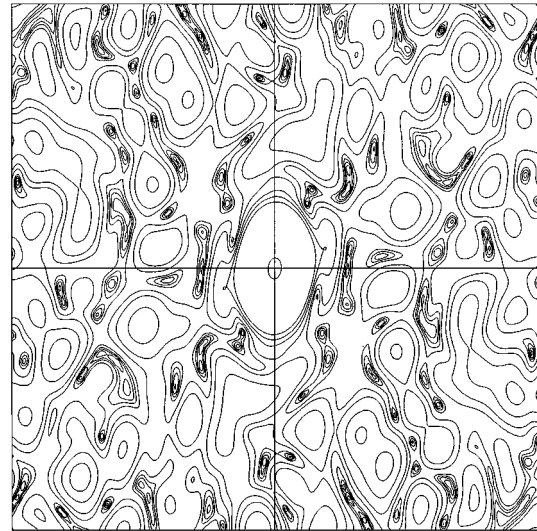
the other ones? The second, more severe one: there is only very little diffuse scattering and, therefore, no stacking disorder and moreover a very high occupation density in the columns of atoms which belong to the vertex defining 20 Å clusters.

The second possible explanation is the following: The random tiling hypothesis explains the stability of the quasicrystal phases by the positive entropy density of the tilings. If this density is high enough and the necessary temperatures are well below the melting point this can lead to a minimum in the free energy and thus to a stabilization of the phase. The nature of the entropy is thought to be purely phasonic, i.e., the entropy is due to a possible rearrangement of tiles by phasonic flips, zipper-moves, etc.¹⁶ The typical range of entropy densities of 2D tilings is 0.1–0.8 per vertex. Theoretical³⁰ and experimental²⁸ observations suggest that only a small number of atoms (in comparison to the number of atoms per tile) must move to generate a flip in the tiling. Typically only 1/10 must move distances of 1–2 Å. Therefore, the realistic scale for the entropy density of a 2D system is 0.01–0.08.

However, there is another natural source of entropy which is not only restricted to quasicrystals and has nothing to do with any tiling scenario: chemical entropy by chemical (and *not* geometrical) disorder. A rough estimate may be the following: Take any lattice and assume chemical disorder only



(a)



(b)

FIG. 16. Absolute value of the Fourier transformation of the internal coordinates of the fivefold phase (Fig. 6) and its contour plot.

for the Co and Ni atoms in the basic Ni-rich structure (e.g., Al₇₀Co₁₁Ni₁₉): The entropy density of this Bernoulli-System is given by:³¹

$$-0.30 \left[\frac{11}{30} \ln \left(\frac{11}{30} \right) + \frac{19}{30} \ln \left(\frac{19}{30} \right) \right] \approx 0.20. \quad (2)$$

This rough estimate shows that chemical disorder can give an amount of entropy that is at least comparable to the possible entropy contribution of random tilings.

A possible explanation for the existence of an ideal quasicrystalline tiling as a high-temperature phase of random tilings is that the chemical entropy density is higher than the phasonic one. In this case, the loss of entropy which will occur by a transition from the geometrically disordered random tiling to the geometrically ordered ideal quasicrystalline state will be more than compensated by the gain of entropy by chemical disorder. The suggestion of the existence of such a transformation is supported by electron-diffraction patterns of the different Al-Co-Ni phases. In all random variants we find diffuse background scattering intensities within the tenfold and diffuse layers between the Bragg layers in the twofold diffraction patterns. This is partially also due to stacking disorder as has already been mentioned. By contrast, we observe nearly no diffuse scattering and no diffuse layers in the case of the basic Ni-rich phase. One simple

mechanism to gain geometrical order is the healing of a linear stacking defect by glueing together two columns separated by a phason flip. This process leads to higher order, and it can create chemical disorder if the two columns have different chemical compositions.

To be precise: We do not have any experimental or theoretical proof for our suggestion, but several facts that fit. The observation of an ideal quasiperiodic tiling (with defects) obtained from a pure high-temperature phase as well as the transition with an increase of temperature from a random tiling phase to this ideal state needs new interpretations.

ACKNOWLEDGMENTS

It is a pleasure to thank M. Baake, M. Schlottmann, V. Elser, C. L. Henley, H.-U. Nissen, M. Scheffer, T. Gödecke, and R. Lück for discussions and helpful comments. Financial support from Deutsche Forschungsgemeinschaft, the Swiss National Science Foundation and the Japanese Science and Technology Corporation is gratefully acknowledged. D.J. wants to thank the Tübingen Group for many years of stimulating work on the theory of quasicrystals and the computing staff of the Materials Science Center, Cornell University, for support.

*Present address: JST, Institute for Materials Research, Tohoku University, Sendai, Japan.

¹D. Shechtman, I. Blech, D. Gratias, and J. W. Cahn, *Phys. Rev. Lett.* **53**, 1951 (1984).

²T. Ishimasa, H.-U. Nissen, and Y. Fukano, *Phys. Rev. Lett.* **55**, 511 (1985).

³L. Bendersky, *Phys. Rev. Lett.* **55**, 1461 (1985).

⁴N. Wang, H. Chen, and K. H. Kuo, *Phys. Rev. Lett.* **59**, 1010 (1987).

⁵X. Z. Li, R. C. Yu, K. H. Kuo, and K. Hiraga, *Philos. Mag. Lett.* **73**, 255 (1996); M. Saito, M. Tanaka, A. P. Tsai, A. Inoue, and T. Masumoto, *Jpn. J. Appl. Phys.* **31**, L109 (1992).

⁶S. Ritsch, C. Beeli, and H.-U. Nissen, *Philos. Mag. Lett.* **74**, 203 (1996).

⁷R. Penrose, *Bull. Inst. Math. Appl.* **10**, 266 (1974).

⁸P. Kramer and R. Neri, *Acta Crystallogr. Sect. A* **40**, 580 (1984).

⁹M. Baake and M. Schlottmann, in *Quasicrystals*, edited by C. Janot and R. Mosseri (World Scientific, Singapore, 1995), p. 15, and references therein.

¹⁰*The Mathematics of Aperiodic Order*, edited by R. V. Moody (Kluwer, Dordrecht, 1997), for an overview.

¹¹*Quasicrystals* (Ref. 9), for an overview.

¹²V. Elser, *Phys. Rev. Lett.* **54**, 1730 (1985).

¹³K. Ingersent, in *Quasicrystals—The State of the Art*, edited by D. P. DiVincenzo and P. J. Steinhardt (World Scientific, Singapore, 1991), p. 185.

¹⁴F. Gähler and H.-C. Jeong, *J. Phys. A* **28**, 1807 (1995).

¹⁵S. E. Burkov, *Phys. Rev. B* **47**, 12 325 (1993).

¹⁶C. L. Henley, in *Quasicrystals—The State of the Art* (Ref. 13), p. 429.

¹⁷D. Joseph and M. Baake, *J. Phys. A* **29**, 6709 (1996).

¹⁸S. Ritsch, Ph.D. thesis, ETH, Zürich, 1996.

¹⁹S. Ritsch, C. Beeli, H.-U. Nissen, T. Gödecke, M. Scheffer and R. Lück, *Philos. Mag. Lett.* **74**, 99 (1996).

²⁰B. Grünbaum and G. C. Shephard, *Tilings and Patterns* (Freeman, New York, 1987).

²¹K. Edagawa, M. Ichihara, K. Suzuki, and S. Takeuchi, *Philos. Mag. Lett.* **66**, 19 (1992).

²²S. Ritsch, C. Beeli, H.-U. Nissen, and R. Lück, *Philos. Mag. A* **71**, 671 (1995).

²³K. Niizeki, *J. Phys. Soc. Jpn.* **63**, 4035 (1994).

²⁴K. Edagawa, H. Sawa, M. Ichihara, K. Suzuki, and S. Takeuchi, *Mater. Sci. Forum* **150 & 151**, 223 (1994).

²⁵H. Chen, S. E. Burkov, Y. He, S. J. Poon, and G. J. Shiflet, *Phys. Rev. Lett.* **65**, 72 (1990).

²⁶H. Selke, C. Pohla, R. Hory, and P. L. Ryder (unpublished).

²⁷H. Bauer, *Wahrscheinlichkeitstheorie* (de Gruyter, Berlin, 1991).

²⁸S. Ritsch, C. Beeli, and H.-U. Nissen, *Phys. Rev. Lett.* **76**, 2507 (1996).

²⁹L. J. Shaw, V. Elser, and C. L. Henley, *Phys. Rev. B* **43**, 3423 (1991).

³⁰G. Zeger and H.-R. Trebin, *Phys. Rev. B* **54**, R720 (1996).

³¹R. Balian, *From Microphysics to Macrophysics* (Springer, Berlin, 1991), Vol. 1.